J. Non-Newtonian Fluid Mech. 158 (2009) 162–169

Contents lists available at ScienceDirect

Journal of Non-Newtonian Fluid Mechanics

journal homepage: www.elsevier.com/locate/jnnfm

Weakly compressible Poiseuille flows of a Herschel–Bulkley fluid

Eleni Taliadorou [a], Georgios C. Georgiou [a,*], Irene Moulitsas [b]

[a] Department of Mathematics and Statistics, University of Cyprus, P.O. Box 20537, 1678 Nicosia, Cyprus
[b] The Cyprus Institute, 17 Kypranoros Street, 1061 Nicosia, Cyprus

ARTICLE INFO

Article history:
Received 28 September 2008
Received in revised form
14 November 2008
Accepted 17 November 2008

Keywords:
Poiseuille flow
Herschel–Bulkley fluid
Compressibility
Equation of state

ABSTRACT

In this work, we derive approximate semi-analytical solutions of the steady, creeping, weakly compressible plane and axisymmetric Poiseuille flows of a Herschel–Bulkley fluid. Since the flow is weakly compressible, the radial velocity component is assumed to be zero and the derivatives of the axial velocity with respect to the axial direction are assumed to be much smaller than those with respect to the radial direction. The axial velocity is then given by an expression similar to that holding for the incompressible flow, the only difference being that the pressure-gradient is a function of the axial coordinate and satisfies a non-linear equation involving the density of the fluid. In the present work, a linear as well as an exponential equation of state, relating the density of the fluid to the pressure, are considered. The pressure distribution along the flow direction is calculated by means of numerical integration and the two-dimensional axial velocity can then be constructed. The effects of compressibility, the equation of state, the Bingham number and the power-law exponent on the solutions are investigated.

1. Introduction

Laminar Poiseuille flows of weakly compressible materials have gained interest in the past two decades due to their applications in many processes involving liquid flows in relatively long tubes, such as waxy crude oil transport [1,2] and polymer extrusion [3,4]. Numerical solutions of weakly compressible Poiseuille flows have been reported for Newtonian fluids [3], generalized Newtonian fluids, such as the Carreau fluid [4] and the Bingham plastic [1], as well as for viscoelastic fluids [5].

The objective of the present work is to solve approximately the plane and axisymmetric Poiseuille flows of weakly compressible fluids with yield stress, i.e. fluids obeying the Herschel–Bulkley constitutive equation, and investigate the effects of compressibility by means of two different equations of state, i.e. a linear and an exponential one. A linear equation of state has been employed in previous numerical studies of the extrudate swell flow [6,7] by Hatzikiriakos and Dealy [8] for HDPE, also for laminar capillary flow by Venerus [9] for compressible Newtonian fluids, and in our previous studies concerning the simulation of the stick-slip extrusion instability [3,4]. Exponential equations of state have been employed, for example, by Ranganathan et al. [10] for a HDPE and, more recently, by Vinay et al. [1] in simulations of weakly compressible Bingham flows.

The paper is organized as follows. In Section 2, the governing equations for the axisymmetric Poiseuille flow are presented and the assumptions under which these are simplified are discussed. Analytical and semi-analytical results are presented for both the incompressible and compressible flows of a Herschel–Bulkley fluid and the numerical method is briefly discussed. In Section 3, the numerical results for the compressible flows of Newtonian, power-law, Bingham, and Herschel–Bulkley fluids with both linear and exponential equations of state are compared and the effects of the compressibility and the yield stress are investigated. Finally, Section 4 contains the conclusions.

2. Governing equations

Let us consider the steady, compressible axisymmetric Poiseuille flow of a generalized Newtonian fluid. The geometry of the flow is given in Fig. 1. Assuming that the flow is creeping and neglecting gravity, the momentum equation is reduced to

$$-\nabla p + \nabla \cdot \boldsymbol{\tau} = 0 \tag{1}$$

where p is the pressure and $\boldsymbol{\tau}$ is the stress tensor. Let us also denote the velocity vector by $\mathbf{u}$ and the rate-of-strain tensor by $\dot{\boldsymbol{\gamma}}$, i.e.

$$\dot{\boldsymbol{\gamma}} \equiv \nabla \mathbf{u} + (\nabla \mathbf{u})^T, \tag{2}$$

where $\nabla \mathbf{u}$ is the velocity-gradient tensor, and the superscript T denotes its transpose. Under the assumption of zero bulk viscosity, which implies that the viscosity forces are only due to shear and not to volume variations [1], the viscous stress tensor for a generalized Newtonian fluid is defined by a constitutive equation of the

* Corresponding author. Tel.: +357 22892612; fax: +357 22892601.
E-mail address: georgios@ucy.ac.cy (G.C. Georgiou).

0377-0257/$ – see front matter © 2008 Elsevier B.V. All rights reserved.
doi:10.1016/j.jnnfm.2008.11.010

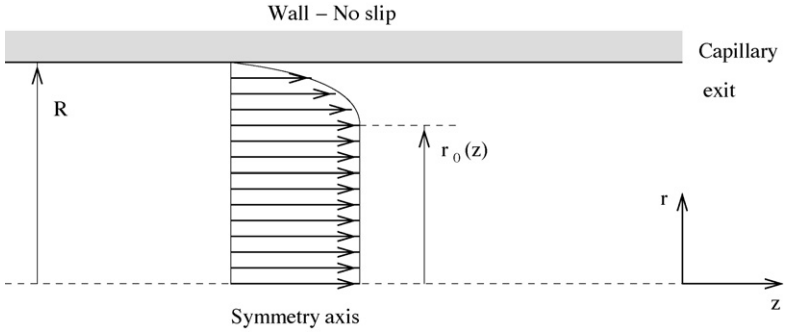

Fig. 1. Geometry of compressible axisymmetric Poiseuille flow of a Herschel–Bulkley fluid.

following general form:

$$\boldsymbol{\tau} = \eta(\dot{\gamma})(\dot{\boldsymbol{\gamma}} - \tfrac{2}{3}\nabla \cdot \mathbf{u}\mathbf{I}), \tag{3}$$

where $\mathbf{I}$ is the identity tensor, and η is the viscosity which depends on the magnitude $\dot{\gamma}$ of the rate-of-strain tensor:

$$\dot{\gamma} = \sqrt{\tfrac{1}{2}II_{\dot{\boldsymbol{\gamma}}}} = \sqrt{\tfrac{1}{2}\dot{\boldsymbol{\gamma}} : \dot{\boldsymbol{\gamma}}} \tag{4}$$

II being the second invariant of a tensor.

The tensorial form of the Herschel–Bulkley constitutive equation is:

$$\begin{cases} \dot{\boldsymbol{\gamma}} = \mathbf{0}, & \tau \le \tau_0 \\ \boldsymbol{\tau} = \left(\dfrac{\tau_0}{\dot{\gamma}} + k\dot{\gamma}^{n-1}\right)\dot{\boldsymbol{\gamma}}, & \tau \ge \tau_0 \end{cases} \tag{5}$$

where τ_0 is the yield stress, k is the consistency index, n is the power law exponent, and τ is the magnitude of the stress tensor. The power-law fluid and the Bingham plastic are the special cases of the Herschel–Bulkley model for τ_0=0 and $n = 1$, respectively.

For a weakly compressible flow, we can assume that the radial velocity component is zero. This assumption is consistent up to first order with Newtonian perturbation solutions in terms of compressibility [11,9]. When $u_r = 0$ the expression for $\dot{\gamma}$ is simplified as follows:

$$\dot{\gamma} = \sqrt{2\left(\frac{\partial u_z}{\partial z}\right)^2 + \left(\frac{\partial u_z}{\partial r}\right)^2} \tag{6}$$

We further assume that $\partial u_z/\partial z \ll 1$ so that the second term in the RHS of Eq. (3) is negligible and

$$\dot{\gamma} \simeq \left|\frac{\partial u_z}{\partial r}\right|. \tag{7}$$

Then from the r-momentum equation it is deduced that $p = p(z)$ and the z-momentum equation is reduced to

$$-\frac{\mathrm{d}p}{\mathrm{d}z} + \frac{1}{r}\frac{\partial}{\partial r}(r\tau_{rz}) = 0, \tag{8}$$

where the pressure-gradient is also a function of z. It should be noted that the above assumptions are valid when the radius of the tube is much smaller than its length [12]. Eq. (5) is simplified as follows:

$$\begin{cases} \dfrac{\partial u_z}{\partial r} = 0, & |\tau_{rz}| \le \tau_0 \\ \tau_{rz} = -\tau_0 + k\left(-\dfrac{\partial u_z}{\partial r}\right)^n, & |\tau_{rz}| \ge \tau_0 \end{cases} \tag{9}$$

Being a function of the pressure, the density also varies across the tube, i.e. $\rho = \rho(z)$. For the mass to be conserved, it must be

$$2\pi\rho(z)\int_0^R u_z(r,z)r\,\mathrm{d}r = \text{const.}$$

or

$$\rho(z)Q(z) = Q_0 \tag{10}$$

where $Q(z)$ is the volumetric flow rate and $Q_0 = Q(0)$.

In the following subsections we will first discuss the one-dimensional incompressible and then the two-dimensional compressible axisymmetric Poiseuille flow of a Herschel–Bulkley fluid. The equations for the planar compressible Poiseuille flow are given in Appendix A.

2.1. Incompressible axisymmetric Poiseuille flow

The solution of the incompressible Poiseuille flow of a Herschel–Bulkley fluid is straightforward and well known. However, it is presented here in order to show the analogy with the weakly compressible solution and to introduce the non-dimensionalization of the problem. In incompressible flow, the pressure-gradient and the density are constant and the axial velocity component depends only on the radial coordinate [13]:

$$u_z(r) = \frac{n}{2^{1/n}(n+1)k^{1/n}}\left(-\frac{\mathrm{d}p}{\mathrm{d}z}\right)^{1/n} \times \begin{cases} (R-r_0)^{1/n+1}, & 0 \le r \le r_0 \\ [(R-r_0)^{1/n+1} - (r-r_0)^{1/n+1}], & r_0 \le r \le R \end{cases} \tag{11}$$

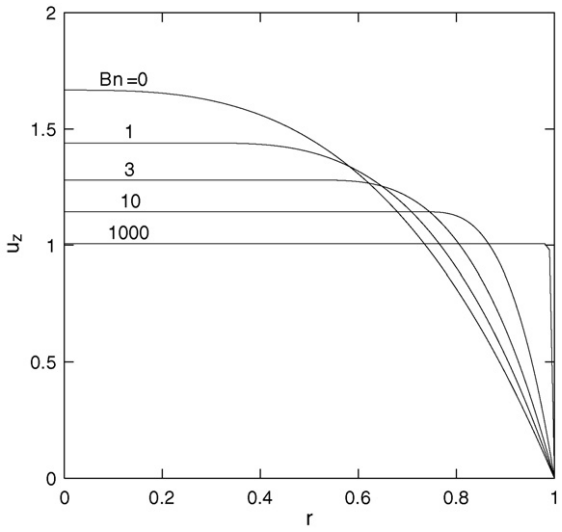

Fig. 2. Velocity profiles for the axisymmetric incompressible Poiseuille flow of a Herschel–Bulkley fluid with $n = 0.5$ and various Bingham numbers.

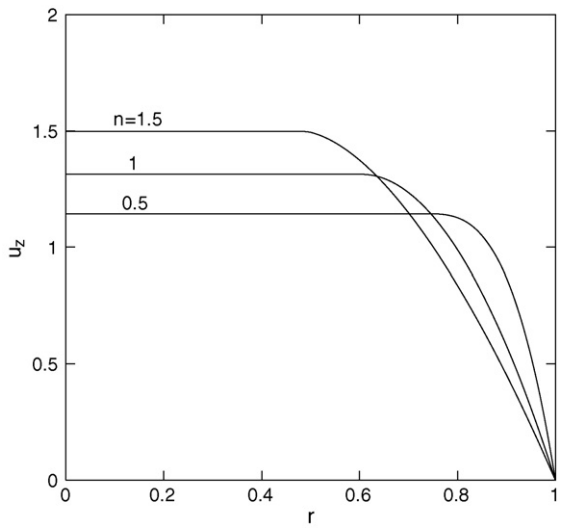

Fig. 3. Velocity profiles for the axisymmetric incompressible Poiseuille flow of a Herschel–Bulkley fluid with $Bn = 10$ and various values of the power-law exponent.

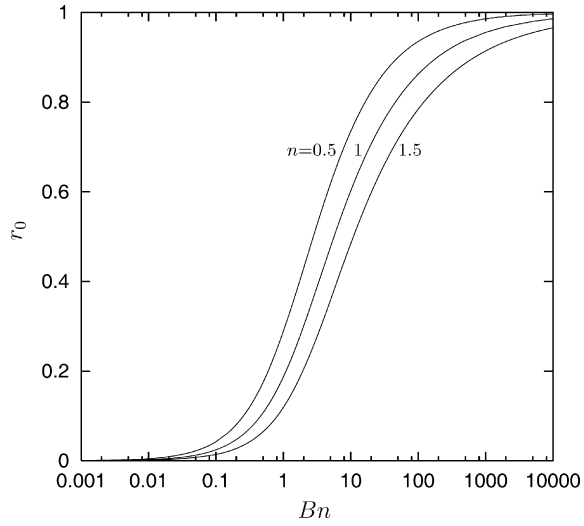

Fig. 4. Position of the yield point in axisymmetric incompressible Poiseuille flow of Herschel–Bulkley fluids.

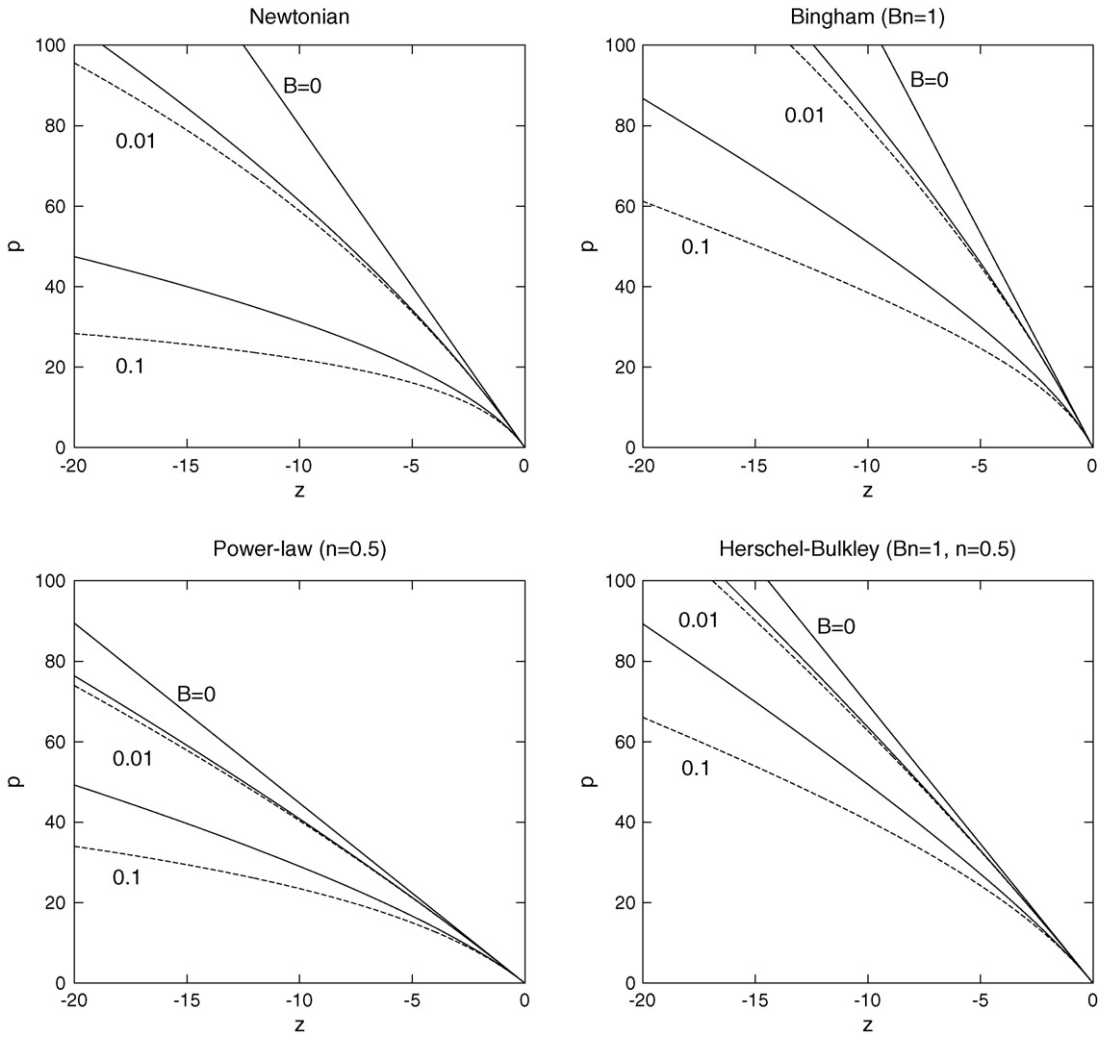

Fig. 5. Pressure distributions for four different fluids obtained with the linear (solid) and the exponential (dashed) equations of state in axisymmetric Poiseuille flow with $B = 0$ (incompressible flow), 0.01 and 0.1.

where R is the capillary radius, $(-dp/dz)$ is the constant pressure-gradient, and

$$r_0 = \frac{2\tau_0}{(-dp/dz)} < R \tag{12}$$

denotes the yield point, i.e. the point at which the material yields. Note that flow occurs only if $(-dp/dz) > 2\tau_0/R$. The volumetric flow rate is given by

$$Q = \frac{\pi n}{2^{1/n}(3n+1)k^{1/n}}\left(-\frac{dp}{dz}\right)^{1/n} R^{1/n+3}\left(1-\frac{r_0}{R}\right)^{1/n+1} \times \left\{1+\frac{2n}{2n+1}\frac{r_0}{R}\left[1+\frac{n}{n+1}\frac{r_0}{R}\right]\right\}. \tag{13}$$

In the cases of a Bingham plastic ($n = 1$) and a power-law fluid ($\tau_0 = 0$, $r_0 = 0$), Eq. (13) is reduced to

$$Q = \frac{\pi}{8k}\left(-\frac{dp}{dz}\right)R^4\left[1-\frac{4}{3}\frac{r_0}{R}+\frac{1}{3}\left(\frac{r_0}{R}\right)^4\right] \tag{14}$$

and

$$Q = \frac{\pi n}{2^{1/n}(3n+1)k^{1/n}}\left(-\frac{dp}{dz}\right)^{1/n} R^{1/n+3} \tag{15}$$

respectively.

In what follows, it is preferable to work with dimensionless equations. Lengths are scaled by the tube radius, R, the velocity by the mean velocity, V_0, in the capillary, and the pressure by kV_0^n/R^n. With these scalings, the dimensionless velocity profile is written as follows:

$$u_z(r) = \frac{n}{2^{1/n}(n+1)}\left(-\frac{dp}{dz}\right)^{1/n} \times \begin{cases} (1-r_0)^{1/n+1}, & 0 \le r \le r_0 \\ [(1-r_0)^{1/n+1} - (r-r_0)^{1/n+1}], & r_0 \le r \le 1 \end{cases} \tag{16}$$

where all quantities are now dimensionless,

$$r_0 = \frac{2Bn}{(-dp/dz)} < 1 \tag{17}$$

and

$$Bn = \frac{\tau_0 R^n}{kV_0^n} \tag{18}$$

is the Bingham number. The dimensionless version of the constitutive equation, i.e. of Eq. (9), is:

$$\begin{cases} \dfrac{\partial u_z}{\partial r} = 0, & |\tau_{rz}| \le Bn \\ \tau_{rz} = -Bn + \left(-\dfrac{\partial u_z}{\partial r}\right)^n, & |\tau_{rz}| \ge Bn \end{cases} \tag{19}$$

Moreover, the dimensionless pressure-gradient is a solution of the following equation:

$$2^{1/n}\frac{3n+1}{n}\left(-\frac{dp}{dz}\right)^3 = \left[\left(-\frac{dp}{dz}\right)-2Bn\right]^{1/n+1}\left[\left(-\frac{dp}{dz}\right)^2 + \frac{4nBn}{2n+1}\left(-\frac{dp}{dz}\right)+\frac{8n^2Bn^2}{(n+1)(2n+1)}\right]. \tag{20}$$

In the case of a power-law fluid ($Bn = 0$), the solution of Eq. (20) is simply

$$\left(-\frac{dp}{dz}\right) = 2\left(\frac{3n+1}{n}\right)^n. \tag{21}$$

In the case of a Bingham-plastic ($n = 1$), Eq. (20) is reduced to

$$3\left(-\frac{dp}{dz}\right)^4 - 8(Bn+3)\left(-\frac{dp}{dz}\right)^3 + 16Bn^4 = 0 \tag{22}$$

It should be noted that flow occurs only if $(-dp/dz) > 2Bn$. For given values of Bn and n, Eq. (20) is easily solved for the pressure-gradient using the Newton–Raphson method, and then the velocity profile can be constructed using Eq. (16). In Fig. 2, the velocity profiles calculated for $n = 0.5$ and various Bingham numbers are shown. In Fig. 3, the velocity profiles obtained with $Bn = 10$ and $n = 0.5$, 1 and 1.5 are compared. With fixed volumetric flow rate, the size of the yielded region is reduced as the power-law exponent is increased. This is also shown in Fig. 4, where the yield point r_0 is plotted as a function of the Bingham number for various values of n.

2.2. Compressible axisymmetric Poiseuille flow

In the case of compressible flow, the pressure-gradient and the density are functions of z and so are r_0 and the volumetric flow rate. It is easily deduced then that the dimensionless axial velocity (scaled by the mean velocity, V_0, at the exit of the capillary) is given by

$$u_z(r,z) = \frac{n}{2^{1/n}(n+1)}\left(-\frac{dp}{dz}\right)^{1/n}(z) \times \begin{cases} [1-r_0(z)]^{1/n+1}, & 0 \le r \le r_0 \\ \{[1-r_0(z)]^{1/n+1} - [r-r_0(z)]^{1/n+1}\}, & r_0 \le r \le 1 \end{cases} \tag{23}$$

where

$$r_0(z) = \frac{2Bn}{(-dp/dz)(z)}. \tag{24}$$

It is clear that at the capillary exit ($z = 0$), Eqs. (23) and (24) give the incompressible flow solution.

It should be pointed out that in steady compressible Poiseuille flow $r_0(z)$ is just a convenient idealization and not a real yield point. Since the axial velocity varies along the tube, $\partial u_z/\partial z > 0$ and thus $\dot{\gamma}$ is nonzero, which implies that unyielded regions cannot exist.

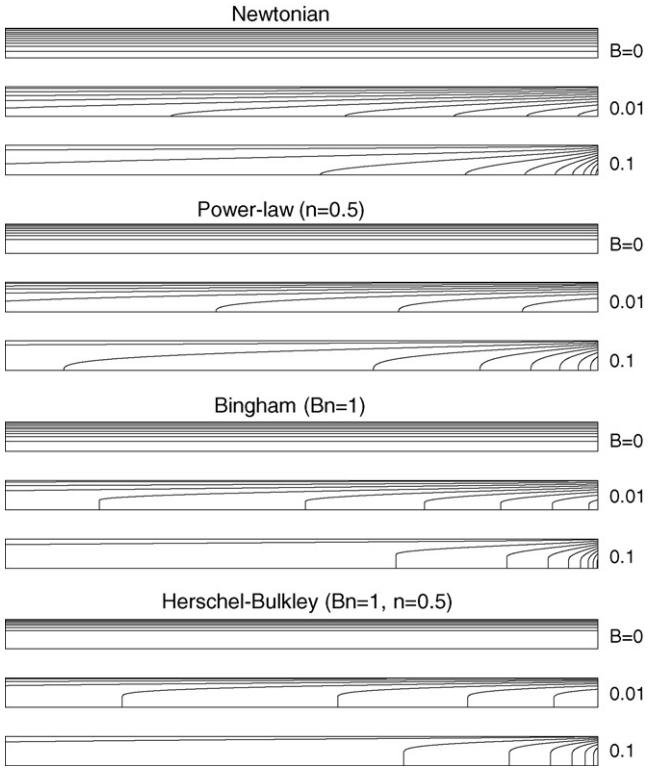

Fig. 6. Velocity contours for four different fluids obtained for the axisymmetric Poiseuille flow with the linear equation of state with $B = 0$ (incompressible flow), 0.01 and 0.1.

Hence, $r_0(z)$ will be referred to as the pseudo-yield point. The fact that the classical plug region flow cannot be obtained in a compressible case was first emphasized by Vinay et al. [1]. However, these authors also calculated steady-state velocity profiles at the inlet and the outlet of the tube with the plug region at the center corresponding to half the pipe radius.

The pressure-gradient $(-\mathrm{d}p/\mathrm{d}z)(z)$ across the capillary, i.e. for $z \leq 0$, can be calculated using the conservation of mass, i.e. Eq. (10). It turns out that the pressure-gradient is a solution of the following equation:

$$2^{1/n}\frac{3n+1}{n\rho(p)}\left(-\frac{\mathrm{d}p}{\mathrm{d}z}\right)^3 = \left[\left(-\frac{\mathrm{d}p}{\mathrm{d}z}\right) - 2Bn\right]^{1/n+1}\left[\left(-\frac{\mathrm{d}p}{\mathrm{d}z}\right)^2 + \frac{4nBn}{2n+1}\left(-\frac{\mathrm{d}p}{\mathrm{d}z}\right) + \frac{8n^2Bn^2}{(n+1)(2n+1)}\right] \quad (25)$$

which involves the pressure-dependent density of the fluid. The pressure-gradient is obviously a function of p and is expected to decrease upstream.

The pressure dependence of the density is taken into account by means of a thermodynamic equation of state. At constant temperature and low pressures, the density can be represented by the linear approximation

$$\rho = \rho_0[1 + \beta(p - p_0)], \quad (26)$$

where $\beta \equiv -(\partial\upsilon/\partial p)_{p_0,T}/\upsilon_0$ is the isothermal compressibility assumed to be constant, υ is the specific volume, ρ_0 and υ_0 are, respectively, the density and the specific volume at a reference pressure p_0, and T is the temperature. For comparison purposes, the following exponential equation is also used:

$$\rho = \rho_0\, \mathrm{e}^{\beta(p-p_0)}. \quad (27)$$

This is equivalent to the linear equation of state for sufficiently small values of β and low pressures. A disadvantage of this equation is the fast growth of the density (for high values of β). On the other hand, the linear model may lead to negative values of the density. Obviously more sophisticated equations of state should be used for highly compressible flows. The equations of state are non-dimensionalized scaling the density ρ by ρ_0 and the pressure as above. We thus get

$$\rho = 1 + Bp \quad (28)$$

and

$$\rho = \mathrm{e}^{Bp}, \quad (29)$$

where the reference pressure, p_0, has been set to zero, and B is the compressibility number,

$$B \equiv \frac{\beta k V_0^n}{R^n}. \quad (30)$$

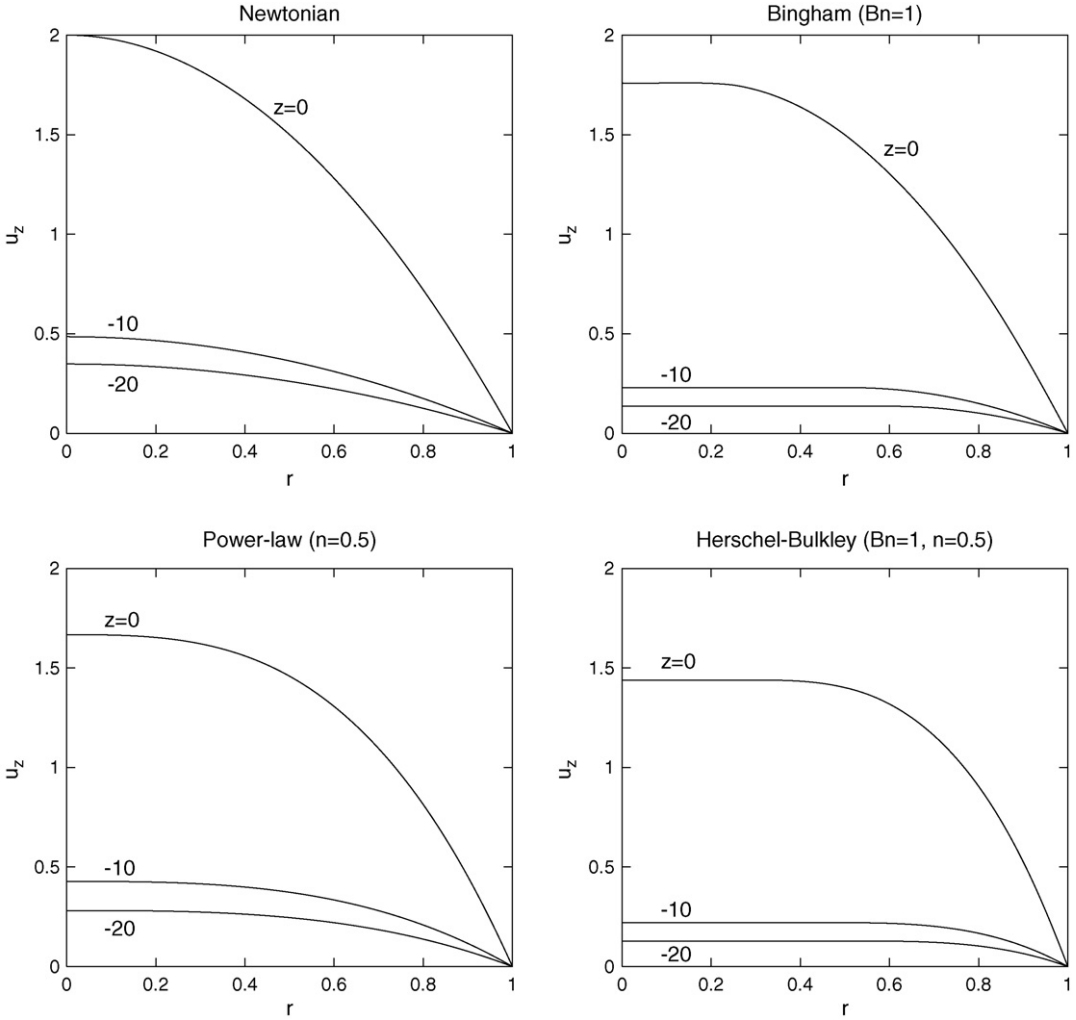

Fig. 7. Velocity profiles at $z = 0, -10$ and -20 for four different fluids obtained with the linear equation of state in axisymmetric Poiseuille flow with $B = 0.1$.

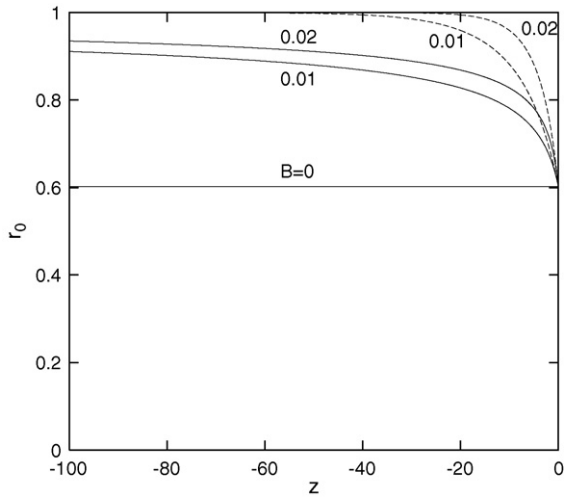

Fig. 8. Position of the pseudo-yield point in axisymmetric Poiseuille flow of a Bingham fluid for $Bn = 10$ and various compressibility numbers. The solid lines correspond to the linear equation of state and the dashed ones to the exponential one.

The Mach number is defined by $Ma = V_0/c$, where c is the speed of sound in the fluid. In the present work, we consider subsonic flows such that $Ma \ll 1$.

Eq. (25) can be integrated analytically in the case of a power-law fluid ($Bn = 0$). With the linear equation of state one finds:

$$p(z) = \frac{1}{B}\left\{\left[1 - 2(n+1)\left(\frac{1}{n}+3\right)^n Bz\right]^{1/(n+1)} - 1\right\} \tag{31}$$

and

$$u_z(r,z) = \frac{(3n+1)(1-r^{1/n+1})}{(n+1)[1-2(n+1)(1/n+3)^n Bz]^{1/(n+1)}} \tag{32}$$

Similarly, with the exponential equation of state one gets:

$$p(z) = \frac{1}{nB}\ln\left[1 - 2n\left(\frac{1}{n}+3\right)^n Bz\right] \tag{33}$$

and

$$u_z(r,z) = \frac{(3n+1)(1-r^{1/n+1})}{(n+1)[1-2n(1/n+3)^n Bz]^{1/n}} \tag{34}$$

Nevertheless, in the general case the pressure-gradient and the pressure are calculated numerically.

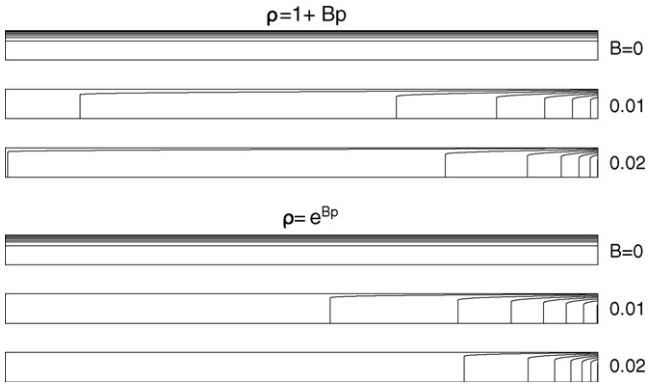

Fig. 9. Velocity contours in axisymmetric Poiseuille flow of a Bingham fluid with $Bn = 10$ and different compressibility numbers using the linear and the exponential equations of state.

Once the pressure $p(z)$ is known at a point (e.g. $p(0) = 0$), the pressure-gradient $(-dp/dz)(z)$ can be calculated from Eq. (25), using the Newton–Raphson method, as before. Hence, we can write

$$-\frac{dp}{dz} = f(p), \tag{35}$$

where the function f is implicitly known. If the pressure p_i at a point z_i is given, then the point z_{i+1} at which the pressure becomes $p_{i+1} = p_i + \Delta p$ can be found by integrating the above equation:

$$z_{i+1} = z_i - \int_{p_i}^{p_i+\Delta p} \frac{dp}{f(p)}. \tag{36}$$

The integral in the RHS of the above equation was calculated using the composite Simpson's rule with 101 points and $\Delta p = 0.1$. At each integration point, the pressure is known and the corresponding pressure-gradient is calculated solving Eq. (25). It is also clear that we start at the channel exit ($z_0 = 0$) and march to the left, up to any desired distance upstream. The numerical code has been tested against the analytical expressions for the pressure distribution in the case of a power-law fluid.

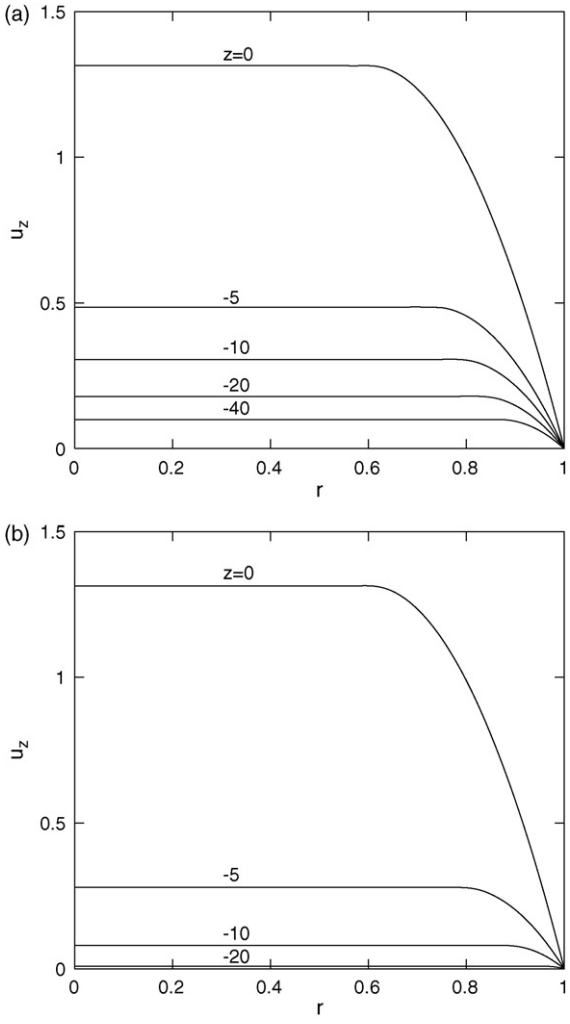

Fig. 10. Velocity profiles at different distances from the capillary exit in axisymmetric Poiseuille flow of a Bingham fluid with $Bn = 10$ and $B = 0.01$: (a) linear equation of state and (b) exponential equation of state.

3. Numerical results

Numerical results have been obtained using both the linear and exponential equations of state in order to investigate the effects of compressibility in Poiseuille flow of fluids with a yield stress. The effects of the three dimensionless parameters controlling the flow, i.e. the Bingham number, the compressibility number, and the power-law exponent have also been studied.

The pressure distributions for a Newtonian, a power-law, a Bingham and a Herschel–Bulkley fluid obtained using both the equations of state for $B = 0$, 0.01 and 0.1 are shown in Fig. 5. Note that the latter value of B is very high and corresponds to a highly compressible flow; it is used here only for illustration purposes. It is clear that the pressure-gradient and the pressure required to drive the flow are reduced as compressibility is increased and increase with the Bingham number and the power-law exponent. The two equations of state give essentially the same results only for sufficiently low compressibility numbers and/or near the die exit. Therefore, a careful selection of the equation of state is necessary when one studies compressible Poiseuille flow in very long channels.

Once the pressure-gradient is known as a function of z, the two-dimensional axial velocity can be constructed by means of Eq. (23). The velocity contours corresponding to the flows of Fig. 5 are shown in Fig. 6. Since the density becomes higher, the flow decelerates upstream and forces the higher contours to bend towards the symmetry axis. In the case of fluids with a yield stress, this phenomenon is more abrupt, since just before the disappearance of a contour line, this is vertical to the symmetry plane and extends up to the corresponding pseudo-yield point. The results for the Bingham plastic ($n = 1$) and the Herschel–Bulkley fluid ($n = 0.5$) are quite similar. We can clearly observe that the pseudo-yield point moves towards the wall as we move upstream. The velocity profiles for the four fluids at $z = 0$, -10 and -20 obtained using the linear equation of state with $B = 0.1$ are given in Fig. 7. As already mentioned, the presence of unyielded regions in steady compressible viscoplastic flow is only an idealization. However, regions of plug-like flow may still exist as indicated by the steady-state numerical results of Vinay et al. [1].

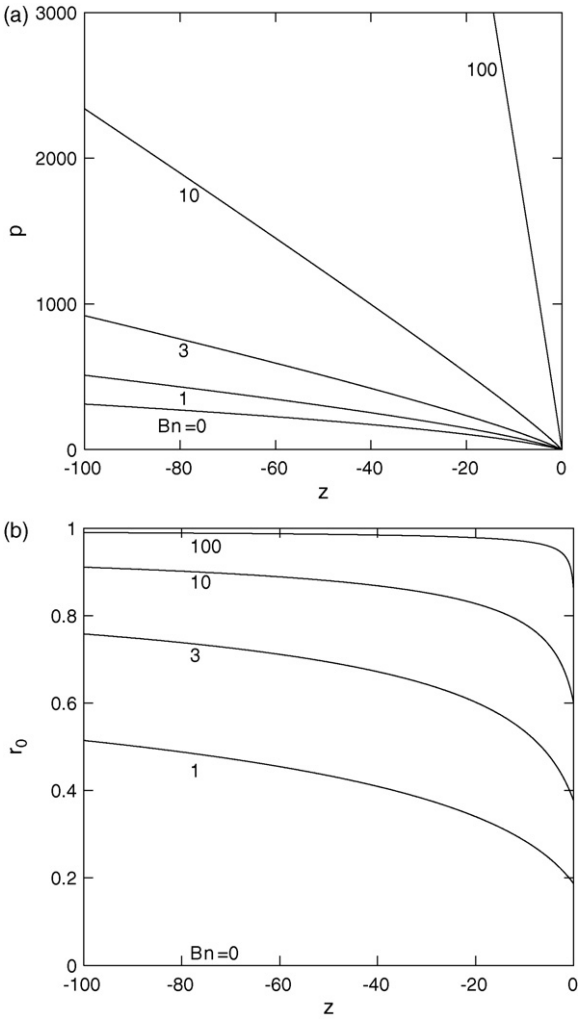

Fig. 11. Effect of the Bingham number in axisymmetric Poiseuille flow of a Bingham fluid with the linear equation of state and $B = 0.01$: (a) pressure distribution and (b) position of the pseudo-yield point.

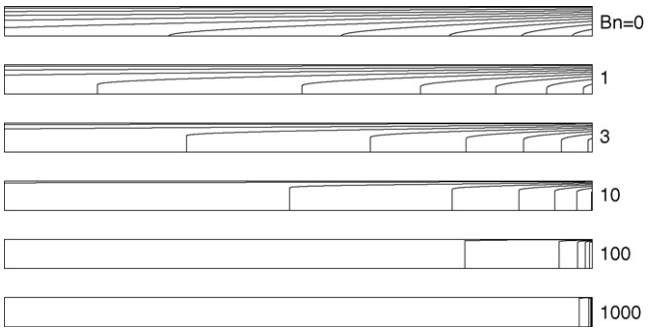

Fig. 12. Effect of the Bingham number on the velocity contours in axisymmetric compressible Poiseuille flow of a Bingham fluid; linear equation of state, $B = 0.01$.

In Fig. 8, the positions of the pseudo-yield point calculated using both equations of state for three compressibility numbers are shown. In the incompressible flow, the yield point is, of course, independent of the axial distance. In the compressible flow, r_0 moves towards the wall as we move upstream, which implies that the size of the plug-like region increases. This phenomenon is better observed in the exponential case due to the faster increase of the density. In Fig. 9, we plot the velocity contours of a Bingham fluid with $Bn = 10$ and $B = 0$, 0.01 and 0.02 using both equations of state. Upstream, the velocity reduces rapidly in the case of the exponential equation of state, which is expected because of the faster increase of the density. As a result, the velocity contours are crowded towards the exit plane. In Fig. 10, we plot the velocity profiles at different distances from the capillary exit of a Bingham fluid with $Bn = 10$ and $B = 0.01$ using again both equations of state.

Fig. 11 shows the effects of the Bingham number on the pressure distribution and the position of the pseudo-yield point in the case of Bingham flow ($n = 1$) using the linear equation of state with $B = 0.01$. We observe that the pressure increases upstream and the pseudo-yield point moves faster towards the wall as the Bingham number increases. This is more clearly shown in Fig. 12, where the velocity contours for different Bingham numbers are shown. As Bn is increased the unyielded region moves towards the exit of the die.

4. Conclusions

We have derived approximate semi-analytical solutions of the axisymmetric and plane Poiseuille flows of weakly compressible Herschel–Bulkley fluid. The two-dimensional axial velocity is given by an expression similar to that for the incompressible flow, with the pressure-gradient and the yield stress point assumed to be functions of the axial coordinate. The pressure-gradient is calculated by means of numerical integration starting at the exit of the tube and marching upstream. The effects of compressibility have been studied by using a linear and an exponential equation of state.

The effects of the yield stress and the power-law exponent on the pressure-gradient and the velocity have also been investigated. Our calculations lead to the following conclusions:

(a) The pressure required to drive the flow for a given tube length is reduced with compressibility.
(b) The linear and the exponential equations of state give similar predictions only for sufficiently low compressibility numbers and/or for short tubes. Hence, the equation of state should be chosen very carefully in numerical simulations of compressible flow in long tubes.
(c) The two-dimensional axial velocity is characterized by plug-like regions the size of which increases upstream, in agreement with the more sophisticated numerical simulations of Vinay et al. [1].
(d) With the exponential equation of state, the upstream growth of the pseudo-unyielded region is much faster than with the linear equation of state.

Appendix A. Compressible plane Poiseuille flow

In plane Poiseuille flow, lengths are scaled by the channel-halfwidth, H, the velocity by the mean velocity, V_0, at the exit of the channel, and the pressure by kV_0^n/H^n. Under the same assumptions used for the axisymmetric flow, the dimensionless velocity profile in the case of compressible plane flow is written as follows:

$$u_x(x,y) = \frac{n}{n+1}\left(-\frac{dp}{dx}\right)^{1/n}(x) \times \begin{cases} [1-y_0(x)]^{1/n+1}, & 0 \le y \le y_0 \\ \{[1-y_0(x)]^{1/n+1} - [y-y_0(x)]^{1/n+1}\}, & y_0 \le y \le 1 \end{cases} \quad (37)$$

where

$$y_0(x) = \frac{Bn}{(-dp/dx)(x)} \quad (38)$$

and

$$Bn = \frac{\tau_0 H^n}{kV_0^n} \quad (39)$$

is the Bingham number. The dimensionless pressure-gradient is a solution of the following equation:

$$\frac{2n+1}{n\rho(p)}\left(-\frac{dp}{dx}\right)^2 = \left[\left(-\frac{dp}{dx}\right) - Bn\right]^{1/n+1}\left[\frac{n}{n+1}Bn + \left(-\frac{dp}{dx}\right)\right]. \quad (40)$$

It is clear that at the channel exit ($x = 0$), Eqs. (37) and (38) yield the solution for incompressible flow.

In the case of a power-law fluid, the solution of Eq. (40) is simply

$$\left(-\frac{dp}{dx}\right) = \left(\frac{2n+1}{n\rho(p)}\right)^n. \quad (41)$$

In the case of a Bingham-plastic, Eq. (40) is reduced to

$$2\left(-\frac{dp}{dx}\right)^3 - 3\left(Bn + \frac{2}{\rho(p)}\right)\left(-\frac{dp}{dx}\right)^2 + Bn^3 = 0, \quad (42)$$

which has the following solution:

$$\left(-\frac{dp}{dx}\right) = \left(\frac{Bn}{2} + \frac{1}{\rho(p)}\right) \times \left[1 + 2\cos\left[\frac{1}{3}\cos^{-1}\left\{1 - \frac{2Bn^3}{(Bn + (2/\rho(p)))^3}\right\}\right]\right]. \quad (43)$$

Detailed results for the compressible plane Poiseuille flow can be found in Ref. [14].

References

[1] G. Vinay, A. Wachs, J.-F. Agassant, Numerical simulation of weakly compressible flows: the restart of pipeline flows of waxy crude oils, J. Non-Newton. Fluid Mech. 136 (2006) 93–105.
[2] M.R. Davidson, Q.D. Nguyen, H.P. Rønningsen, Restart model for a multi-plug gelled waxed oil pipeline, J. Petrol. Sci. Eng. 59 (2007) 1–16.
[3] G.C. Georgiou, M.J. Crochet, Compressible viscous flow in slits with slip at the wall, J. Rheol. 38 (1994) 639–654.
[4] G.C. Georgiou, The time-dependent compressible Poiseuille and extrudate-swell flows of a Carreau fluid with slip at the wall, J. Non-Newton. Fluid Mech. 109 (2003) 93–114.
[5] F. Belblidia, I.J. Keshtiban, M.F. Webster, Stabilised computations for viscoelastic flows under compressible considerations, J. Non-Newton. Fluid Mech. 134 (2006) 56–76.
[6] C.R. Beverly, R.I. Tanner, Compressible extrudate swell, Rheol. Acta 35 (1993) 526–531.
[7] G.C. Georgiou, The compressible Newtonian extrudate swell problem, Int. J. Numer. Methods Fluids 20 (1995) 255–261.
[8] S.G. Hatzikiriakos, J.M. Dealy, Role of slip and fracture in the oscillating flow of a HDPE in a capillary, J. Rheol. 36 (1992) 845–883.
[9] D.C. Venerus, Laminar capillary flow of compressible viscous fluids, J. Fluid Mech. 555 (2006) 59–80.
[10] M. Ranganathan, M.R. Mackley, P.H.J. Spitteler, The application of the multipass rheometer to time-dependent capillary flow measurements of a polyethylene melt, J. Rheol. 43 (1999) 443–451.
[11] L.W. Schwartz, A perturbation solution for compressible viscous channel flows, J. Eng. Math. 21 (1987) 69–86.
[12] G. Vinay, A. Wachs, I. Frigaard, Start-up transients and efficient computation of isothermal waxy crude oil flows, J. Non-Newton. Fluid Mech. 143 (2007) 141–156.
[13] R.R. Huilgol, Z. You, Application of the augmented Lagrangian method to steady pipe flows of Bingham, Casson and Herschel–Bulkley fluids, J. Non-Newton. Fluid Mech. 128 (2005) 126–143.
[14] E. Taliadorou, Numerical simulations of weakly compressible generalized Newtonian flows, Ph.D. Thesis, Department of Mathematics and Statistics, University of Cyprus, 2008.